

# Laser cooling and trapping of neutral atoms

J. Dalibard and C. Cohen-Tannoudji,  
Laboratoire Kastler Brossel\*and Collège de France,  
24 rue Lhomond, 75005 Paris, France

## 1 Introduction

Electromagnetic interactions can be used to act on atoms, to manipulate them, to control their various degrees of freedom. With the development of laser sources, this research field has considerably expanded during the last few years. Methods have been developed to trap atoms and to cool them to very low temperatures. The purpose of this paper is to review the physical processes which are at the basis of this research field, and to present some of its most remarkable applications [1].

Two types of degrees of freedom can be considered for an atom: the internal degrees of freedom, such as the electronic configuration or the spin polarization, in the center of mass system; the external degrees of freedom, which are essentially the position and the momentum of the center of mass. The manipulation of internal degrees of freedom goes back to optical pumping [2], which uses resonant exchanges of angular momentum between atoms and circularly polarized light for polarizing the spins of these atoms. These experiments predate the use of lasers in atomic physics. The manipulation of external degrees of freedom uses the concept of radiative forces resulting from the exchanges of linear momentum between atoms and light. Radiative forces exerted by the light coming from the sun were already invoked by J. Kepler to explain the tails of the comets. Although they are very small when one uses ordinary light sources, these forces were also investigated experimentally in the beginning of this century by P. Lebedev, E. F. Nichols and G. F. Hull, R. Frisch [3].

It turns out that there is a strong interplay between the dynamics of internal and external degrees of freedom. This is at the origin of efficient laser cooling mechanisms, such as *Sisyphus cooling* or *Velocity Selective Coherent Population Trapping*, which were discovered at the end of the 80's (for a historical survey of these developments, see for example [4]). These mecha-

---

\*Unité de Recherche de l'Ecole normale supérieure et de l'Université Pierre et Marie Curie, associée au CNRS.

nisms have allowed laser cooling to overcome important fundamental limits, such as the *Doppler limit* and the *single photon recoil limit*, and to reach the microKelvin, and even the nanoKelvin range.

This paper is organized as follows. In section 2 we briefly review the basic processes which enter into play when an atom modelled as a two-level system interacts with a monochromatic laser beam. Then, in section 3, we introduce the idea of Doppler cooling, and of magneto-optical and dipole trapping. The notions of sub-Doppler and sub-recoil cooling are presented respectively in sections 4 and 5. In section 6 we briefly outline the complementary technique of evaporative cooling and we present its most remarkable achievement, namely the realization of Bose-Einstein condensates with dilute atomic gases. Finally in section 7, we present another very promising application of laser cooled atoms, leading to a spectacular improvement of the performances of atomic clocks.

## 2 Interaction of a Two-Level Atom with a Quasi-Resonant Light Beam

To classify the basic physical processes which are used for manipulating atoms by light, it is useful to distinguish two large categories of effects : dissipative (or absorptive) effects on the one hand, reactive (or dispersive) effects on the other hand. This partition is relevant for both internal and external degrees of freedom.

Consider first a light beam with frequency  $\omega_L$  propagating through a medium consisting of atoms with resonance frequency  $\omega_A$ . The index of refraction describing this propagation has an imaginary part and a real part which are associated with two types of physical processes. The incident photons can be absorbed, more precisely scattered in all directions. The corresponding attenuation of the light beam is maximum at resonance. It is described by the imaginary part of the index of refraction which varies with  $\omega_L - \omega_A$  as a Lorentz absorption curve. We will call such an effect a dissipative (or absorptive) effect. The speed of propagation of light is also modified. The corresponding dispersion is described by the real part  $n$  of the index of refraction whose difference from 1,  $n - 1$ , varies with  $\omega_L - \omega_A$  as a Lorentz dispersion curve. We will call such an effect a reactive (or dispersive) effect. Dissipative effects and reactive effects also appear for the atoms, as a result of their interaction with photons. Consider for simplicity an atom sitting in point  $\mathbf{r}$ , which can be modelled by a two-level system involving a ground state  $g$  and an excited state  $e$ , with a radiative lifetime  $\Gamma^{-1}$  (see figure 1). For relatively low laser intensities, these dissipative and reactive effects can be understood as a broadening and a shift of the atomic ground state. The broadening  $\Gamma'$  is the rate at which photons are scattered from the incident beam by the atom. The shift  $\hbar\Delta'$  is the energy displacement of the ground

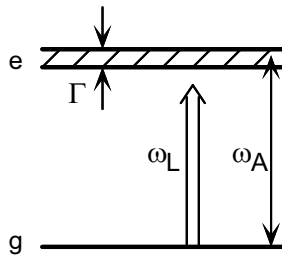


Figure 1: Modelling of an atomic transition in terms of a two-level system.

level, as a result of virtual absorptions and stimulated emissions of photons by the atom within the light beam mode; it is called light-shift or AC Stark shift. The expressions for  $\Gamma'$  and  $\Delta'$  can be derived in various ways, using either the optical Bloch equation formalism or the dressed atom approach [5]. We simply give here the results, as functions of the local intensity  $I(\mathbf{r})$  of the light beam, the saturation intensity  $I_s$ , and the detuning  $\Delta = \omega_L - \omega_A$ :

$$\Gamma'(\mathbf{r}) = \Gamma \frac{I(\mathbf{r})}{2I_s} \frac{1}{1 + 4\Delta^2/\Gamma^2} \quad \Delta'(\mathbf{r}) = \Delta \frac{I(\mathbf{r})}{2I_s} \frac{1}{1 + 4\Delta^2/\Gamma^2} \quad (1)$$

These expressions are valid as long as  $\Gamma'$  and  $\Delta'$  are respectively small compared with  $\Gamma$  and  $\Delta$ . The saturation intensity for a typical atomic resonance transition is quite low, in regard of the intensities achievable with usual laser sources. For instance, for the resonance line of sodium atoms, one gets  $I_s = 6 \text{ mW cm}^{-2}$ .

Both  $\Gamma'$  and  $\Delta'$  are proportional to the light intensity. They vary with the detuning as Lorentz absorption and dispersion curves, respectively, which justifies the denominations absorptive and dispersive used for these two types of effects. For large detunings ( $|\Delta| \gg \Gamma$ ),  $\Gamma'$  varies as  $1/\Delta^2$  and becomes negligible compared to  $\Delta'$  which varies as  $1/\Delta$ . On the other hand, for small detunings, ( $|\Delta| \ll \Gamma$ ),  $\Gamma'$  is much larger than  $\Delta'$ . In the high intensity limit, the expressions (1) are not valid anymore, and the physical understanding of the atom-laser interaction is more subtle [5]. Let us simply indicate that in this case the atomic scattering rate saturates to the value  $\Gamma/2$ , indicating that the average population of the atomic excited state reaches  $1/2$ .

### 3 Radiative Forces on a Two-Level Atom

#### 3.1 The two types of radiative forces

There are two types of radiative forces, associated respectively with dissipative and reactive effects.

Dissipative forces, also called radiation pressure forces or scattering forces, are associated with the transfer of linear momentum from the incident light beam to the atom in resonant scattering processes. They are proportional to the scattering rate  $\Gamma'$ . Consider for example an atom in a laser plane wave with wave vector  $\mathbf{k}$ . Because photons are scattered with equal probabilities in two opposite directions, the mean momentum transferred to the atom in an absorption-spontaneous emission cycle is equal to the momentum  $\hbar\mathbf{k}$  of the absorbed photon. The mean rate of momentum transfer, *i.e.* the mean force, is thus equal to  $\hbar\mathbf{k}\Gamma'$ . Since  $\Gamma'$  saturates to  $\Gamma/2$  at high intensity, the radiation pressure force saturates to  $\hbar\mathbf{k}\Gamma/2$ . The corresponding acceleration (or deceleration) which can be communicated to an atom with mass  $M$ , is equal to  $a_{\max} = \hbar k\Gamma/2M = v_R/2\tau$ , where  $v_R = \hbar k/M$  is the recoil velocity of the atom absorbing or emitting a single photon, and  $\tau = 1/\Gamma$  is the radiative lifetime of the excited state. For sodium atoms,  $v_R = 3 \times 10^{-2}\text{m s}^{-1}$  and  $\tau = 1.6 \times 10^{-9}\text{s}$ , so that  $a_{\max}$  can reach values as large as  $10^6\text{m s}^{-2}$ , *i.e.*  $10^5g$  where  $g$  is the acceleration due to gravity. With such a force, one can stop a thermal atomic beam in a distance of the order of one meter, provided that one compensates for the Doppler shift of the decelerating atom, by using for example a spatially varying Zeeman shift [6] or a chirped laser frequency [7].

Dispersive forces, also called dipole forces or gradient forces, can be interpreted in terms of position dependent light shifts  $\hbar\Delta'(\mathbf{r})$  due to a spatially varying light intensity [8]. Consider for example a laser beam well detuned from resonance, so that one can neglect  $\Gamma'$  (no scattering process). The atom thus remains in the ground state and the light shift  $\hbar\Delta'(\mathbf{r})$  of this state plays the role of a potential energy, giving rise to a force which is equal and opposite to its gradient :  $\mathbf{F} = -\nabla[\hbar\Delta'(\mathbf{r})]$ . Such a force can also be interpreted as resulting from a redistribution of photons between the various plane waves forming the laser wave in absorption-stimulated emission cycles. If the detuning is not large enough to allow  $\Gamma'$  to be neglected, spontaneous transitions occur between dressed states having opposite gradients, so that the instantaneous force oscillates back and forth between two opposite values in a random way. Such a dressed atom picture provides a simple interpretation of the mean value and of the fluctuations of dipole forces [9].

### 3.2 Doppler cooling and magneto-optical trapping

The principle of Doppler cooling has been suggested by T.W. Hänsch and A.L. Schawlow [10] for neutral atoms, and by D. Wineland and H. Dehmelt [11] for trapped ions. In the proposal [10] this cooling results from a Doppler induced imbalance between two opposite radiation pressure forces. The two counterpropagating laser waves have the same (weak) intensity and the same frequency. They are slightly detuned to the red of the atomic

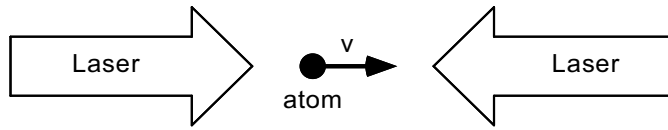


Figure 2: Doppler cooling in 1D, resulting from the imbalance between the radiation pressure forces of two counterpropagating laser waves. The laser detuning is negative ( $\omega_L < \omega_A$ ).

frequency ( $\omega_L < \omega_A$ ) (see fig. 2). For an atom at rest, the two radiation pressure forces exactly balance each other and the net force is equal to zero. For a moving atom, the apparent frequencies of the two laser waves are Doppler shifted. The counterpropagating wave gets closer to resonance and exerts a stronger radiation pressure force than the copropagating wave which gets farther from resonance. The net force is thus opposite to the atomic velocity  $v$  and can be written for small  $v$  as  $F = -\alpha v$  where  $\alpha$  is a friction coefficient. By using three pairs of counterpropagating laser waves along three orthogonal directions, one can damp the atomic velocity in a very short time, on the order of a few microseconds, achieving what is called an *optical molasses* [12].

The Doppler friction responsible for the cooling is necessarily accompanied by fluctuations due to the fluorescence photons which are spontaneously emitted in random directions and at random times. These photons communicate to the atom a random recoil momentum  $\hbar k$ , responsible for a momentum diffusion described by a diffusion coefficient  $D$ . As in usual Brownian motion, competition between friction and diffusion usually leads to a steady-state, with an equilibrium temperature proportional to  $D/\alpha$ . The theory of Doppler cooling [13, 14, 15] predicts that the equilibrium temperature obtained with such a scheme is always larger than a certain limit  $T_D$ , called the Doppler limit, and given by  $k_B T_D = \hbar\Gamma/2$  where  $\Gamma$  is the natural width of the excited state and  $k_B$  the Boltzmann constant. This limit, which is reached for  $\Delta = \omega_L - \omega_A = -\Gamma/2$ , is, for alkali atoms, on the order of  $100 \mu\text{K}$ . In fact, when the measurements became precise enough, it appeared that the temperature in optical molasses was much lower than expected [16]. This indicates that other laser cooling mechanisms, more powerful than Doppler cooling, are operating. We will come back to this point in the next section.

The imbalance between two opposite radiation pressure forces can be also made position dependent through a spatially dependent Zeeman shift produced by a magnetic field gradient. In a one-dimensional configuration, initially proposed by one of us (J.D.), the two counterpropagating waves, which are detuned to the red ( $\omega_L < \omega_A$ ) and which have opposite circular polarizations are in resonance with the atom at different places. This

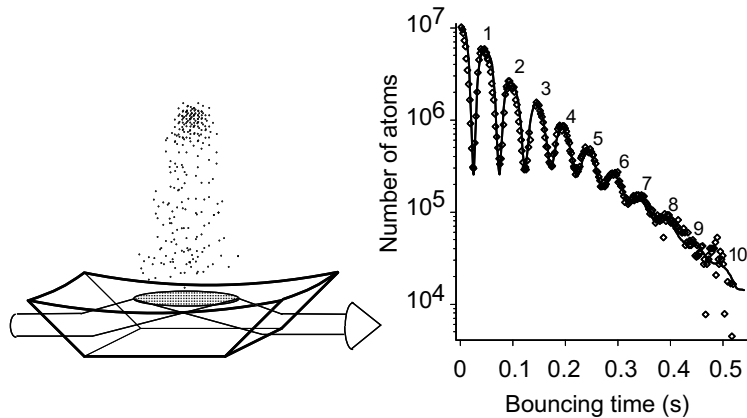


Figure 3: Gravitational cavity for neutral atoms (from [26]). (a) Trampoline for atoms: atoms released from a magneto-optical trap bounce off a concave mirror formed by a blue detuned evanescent wave ( $\omega_L > \omega_A$ ), propagating at the surface of a glass prism. (b) Number of atoms at the apex of the average trajectory, as a function of the time after the magneto-optical trap has been switched off.

results in a restoring force towards the point where the magnetic field vanishes. Furthermore the non zero value of the detuning provides a Doppler cooling. Such a scheme can be extended to three dimensions and leads to a robust, large and deep trap called *magneto-optical trap* (MOT) [17]. It combines trapping and cooling, it has a large velocity capture range and it can be used for trapping atoms in a small cell filled with a low pressure vapour [18].

### 3.3 Dipole traps and atomic mirrors

When the detuning is negative ( $\omega_L < \omega_A$ ), light shifts are negative. If the laser beam is focussed, the focal zone where the intensity is maximum appears as a minimum of potential energy, forming a potential well where sufficiently cold atoms can be trapped [19, 20, 21, 22].

If the detuning is positive, light shifts are positive and can thus be used to produce potential barriers. For example an evanescent blue detuned wave at the surface of a piece of glass can prevent slow atoms impinging on the glass surface from touching the wall, making them bounce off a “carpet of light” [23]. This is the principle of mirrors for atoms. Plane atomic mirrors [24, 25] have been realized as well as concave mirrors [26] (see fig. 3).

## 4 Sub-Doppler Cooling

In the previous section, we discussed separately the manipulation of internal and external degrees of freedom, and we have described physical mechanisms involving only one type of physical effect, either dispersive or dissipative. In fact, there exist cooling mechanisms resulting from an interplay between spin and external degrees of freedom, and between dispersive and dissipative effects. We discuss in this section one of them, the so-called ‘‘Sisyphus cooling’’ or ‘‘polarization-gradient cooling’’ mechanism [27, 28], which leads to temperatures much lower than Doppler cooling. One can understand in this way the sub-Doppler temperatures observed in optical molasses [16].

### 4.1 The Sisyphus mechanism

Most atoms, in particular alkali atoms, have a Zeeman structure in the ground state. Since the detuning used in laser cooling experiments is not too large compared to  $\Gamma$ , both differential light shifts and optical pumping transitions exist for the various Zeeman sublevels of the ground state. Furthermore, the laser polarization varies in general in space so that light shifts and optical pumping rates are position-dependent. We show now, with a simple one-dimensional example, how the combination of these various effects can lead to a very efficient cooling mechanism.

Consider the laser configuration of Fig. 4, consisting of two counterpropagating plane waves along the  $z$ -axis, with orthogonal linear polarizations and with the same frequency and the same intensity. Because the phase shift between the two waves varies linearly with  $z$ , the polarization of the total field changes from  $\sigma^+$  to  $\sigma^-$  and vice versa every  $\lambda/4$ . In between, it is elliptical or linear.

Consider now the simple case where the atomic ground state has an angular momentum  $J_g = 1/2$ . The two Zeeman sublevels  $M_g = \pm 1/2$  undergo different light shifts, depending on the laser polarization, so that the Zeeman degeneracy in zero magnetic field is removed. This gives the energy diagram of Fig. 4 showing spatial modulations of the Zeeman splitting between the two sublevels with a period  $\lambda/2$ .

If the detuning  $\Delta$  is not too large compared to  $\Gamma$ , there are also real absorptions of photons by the atom followed by spontaneous emission, which give rise to optical pumping transfers between the two sublevels, whose direction depends on the polarization:  $M_g = -1/2 \longrightarrow M_g = +1/2$  for a  $\sigma^+$  polarization,  $M_g = +1/2 \longrightarrow M_g = -1/2$  for a  $\sigma^-$  polarization. Here also, the spatial modulation of the laser polarization results in a spatial modulation of the optical pumping rates with a period  $\lambda/2$ .

The two spatial modulations of light shifts and optical pumping rates are of course correlated because they are due to the same cause, the spatial modulation of the light polarization. These correlations clearly appear in

Fig. 4. With the proper sign of the detuning, optical pumping always transfers atoms from the higher Zeeman sublevel to the lower one. Suppose now that the atom is moving to the right, starting from the bottom of a valley, for example in the state  $M_g = +1/2$  at a place where the polarization is  $\sigma^+$ . Because of the finite value of the optical pumping time, there is a time lag between internal and external variables and the atom can climb up the potential hill before absorbing a photon and reach the top of the hill where it has the maximum probability to be optically pumped in the other sublevel, i.e. in the bottom of a valley, and so on.

Like Sisyphus in the Greek mythology, who was always rolling a stone up the slope, the atom is running up potential hills more frequently than down. When it climbs a potential hill, its kinetic energy is transformed into potential energy. Dissipation then occurs by light, since the spontaneously emitted photon has an energy higher than the absorbed laser photon. After each Sisyphus cycle, the total energy  $E$  of the atom decreases by an amount of the order of  $U_0$ , where  $U_0$  is the depth of the optical potential wells of Fig. 4. When  $E$  becomes smaller than  $U_0$ , the atom remains trapped in the potential wells.

## 4.2 The limit of Sisyphus cooling

The previous discussion shows that Sisyphus cooling leads to temperatures  $T_{\text{Sis}}$  such that  $k_B T_{\text{Sis}} \simeq U_0$ . According to Eq. (4), the light shift  $U_0$  is proportional to  $I/\Delta$ . Such a dependence of  $T_{\text{Sis}}$  on the laser intensity and on the detuning has been checked experimentally [29].

At low intensity, the light shift is much smaller than  $\hbar\Gamma$ . This explains why Sisyphus cooling leads to temperatures much lower than those achievable with Doppler cooling. One cannot however decrease indefinitely the laser intensity. The previous discussion ignores the recoil due to the spontaneously emitted photons which increase the kinetic energy of the atom by an amount on the order of  $E_R$ , where

$$E_R = \hbar^2 k^2 / 2M \quad (2)$$

is the recoil energy of an atom absorbing or emitting a single photon. When  $U_0$  becomes on the order or smaller than  $E_R$ , the cooling due to Sisyphus cooling becomes weaker than the heating due to the recoil, and Sisyphus cooling no longer works. This shows that the lowest temperatures which can be achieved with such a scheme are on the order of a few  $E_R/k_B$ , which is on the order of a few microKelvins for rubidium or cesium atoms. This result is confirmed by a full quantum theory of Sisyphus cooling [30] and is in good agreement with experimental results.

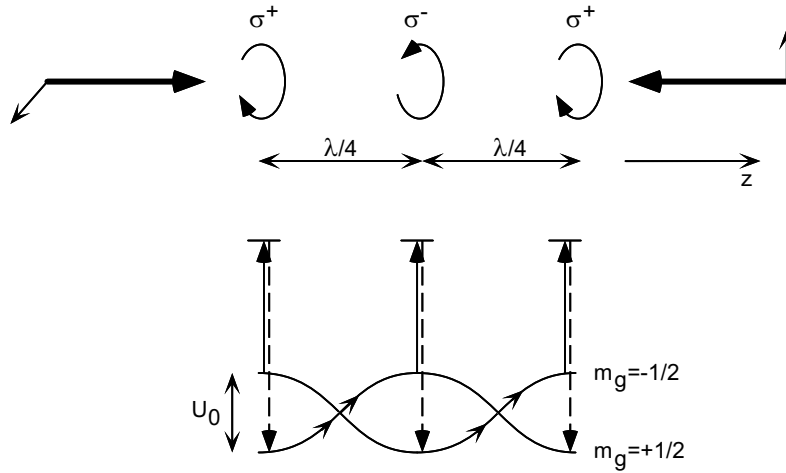


Figure 4: One dimensional Sisyphus cooling. The laser configuration is formed by two counterpropagating waves along the  $z$  axis with orthogonal linear polarizations. The polarization of the resulting field is spatially modulated with a period  $\lambda/2$ . For an atom with two ground Zeeman sublevels  $M_g = \pm 1/2$ , the spatial modulation of the laser polarization results in correlated spatial modulations of the light shifts of these two sublevels and of the optical pumping rates between them. Because of these correlations, a moving atom runs up potential hills more frequently than down.

### 4.3 Optical lattices

For the optimal conditions of Sisyphus cooling, atoms become so cold that they get trapped in the quantum vibrational levels of a potential well. More precisely, one must consider energy bands in this periodic structure [31]. Experimental observation of such a quantization of atomic motion in an optical potential was first achieved in one dimension [32, 33]. Atoms are trapped in a spatial periodic array of potential wells, called a *1D-optical lattice*, with an antiferromagnetic order, since two adjacent potential wells correspond to opposite spin polarizations. 2D and 3D optical lattices have been realized subsequently (see the review papers [34, 35]).

## 5 Sub-Recoil Cooling

### 5.1 How to circumvent the one photon recoil limit

In most laser cooling schemes, fluorescence cycles never cease. Since the random recoil  $\hbar k$  communicated to the atom by the spontaneously emitted

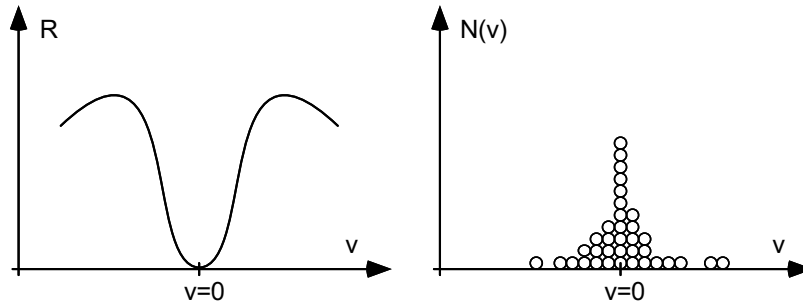


Figure 5: Sub recoil cooling. The random walk in velocity space is characterized by a jump rate vanishing in  $v = 0$ . As a result, atoms which fall in a small interval around  $v = 0$  remain trapped there for a long time.

photons cannot be controlled, it seems impossible to reduce the atomic momentum spread  $\delta p$  below a value corresponding to the photon momentum  $\hbar k$ . The condition  $\delta p = \hbar k$  defines the “single photon recoil limit”, the recoil temperature being set as  $k_B T_R/2 = E_R$ . The value of  $T_R$  ranges from a few hundred nanoKelvin for alkalis to a few microKelvin for metastable helium. It is in fact possible to circumvent this limit and to reach temperatures  $T$  lower than  $T_R$ , a regime called *subrecoil laser cooling*. The basic idea is to create a situation where the photon absorption rate  $\Gamma'$ , which is also the jump rate  $R$  of the atomic random walk in velocity space, depends on the atomic velocity  $v = p/M$  and vanishes for  $v = 0$  (Fig. 5). Consider then an atom with  $v = 0$ . For such an atom, the absorption of light is quenched. Consequently, there is no spontaneous reemission and no associated random recoil. One protects in this way ultracold atoms (with  $v \simeq 0$ ) from the “bad” effects of the light. On the other hand, atoms with  $v \neq 0$  can absorb and reemit light. In such absorption-spontaneous emission cycles, their velocities change in a random way and the corresponding random walk in  $v$  – space can transfer atoms from the  $v \neq 0$  absorbing states into the  $v \simeq 0$  dark states where they remain trapped and accumulate.

Up to now, two subrecoil cooling schemes have been proposed and demonstrated. In the first one, called *Velocity Selective Coherent Population Trapping* (VSCPT), the vanishing of  $R(v)$  for  $v = 0$  is achieved by using destructive quantum interference between different absorption amplitudes [36]. The second one, called Raman cooling, uses appropriate sequences of stimulated Raman and optical pumping pulses for tailoring the appropriate shape of  $R(v)$  [37].

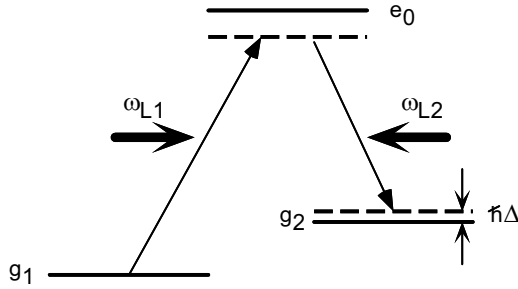


Figure 6: Coherent population trapping. A three level atom is driven by two laser fields. When the detuning  $\Delta$  of the stimulated Raman process is zero, the atom is optically pumped into a linear superposition of  $g_1$  and  $g_2$ , which no longer absorbs light.

## 5.2 Brief survey of VSCPT

We first recall the principle of the quenching of absorption by *coherent population trapping* [38]. Consider the 3-level system of Fig. 6, with two ground state sublevels  $g_1$  and  $g_2$  and one excited sublevel  $e_0$ , driven by two laser fields with frequencies  $\omega_{L1}$  and  $\omega_{L2}$ , exciting the transitions  $g_1 \leftrightarrow e_0$  and  $g_2 \leftrightarrow e_0$ , respectively. Let  $\hbar\Delta$  be the detuning from resonance for the stimulated Raman process consisting of the absorption of one photon  $\omega_{L1}$  and the stimulated emission of one  $\omega_{L2}$  photon, the atom going from  $g_1$  to  $g_2$ . One observes that the fluorescence rate  $R$  vanishes for  $\Delta = 0$ . In this case indeed, atoms are optically pumped into a linear superposition of  $g_1$  and  $g_2$  which is not coupled to  $e_0$  because of a destructive interference between the two absorption amplitudes  $g_1 \rightarrow e_0$  and  $g_2 \rightarrow e_0$ .

The basic idea of VSCPT is to use the Doppler effect for making the detuning  $\Delta$  of the stimulated Raman process of Fig. 6 proportional to the atomic velocity  $v$ . The quenching of absorption by coherent population trapping is thus made velocity dependent and one achieves the situation of Fig. 5. This is obtained by taking the two laser waves  $\omega_{L1}$  and  $\omega_{L2}$  counterpropagating along the  $z$ -axis and by choosing their frequencies in such a way that  $\Delta = 0$  for an atom at rest. Then, for an atom moving with a velocity  $v$  along the  $z$ -axis, the opposite Doppler shifts of the two laser waves result in a Raman detuning  $\Delta = (k_1 + k_2)v$  proportional to  $v$ .

A more quantitative analysis of the cooling process [39] shows that the dark state, for which  $R = 0$ , is a linear superposition of two states which differ not only by the internal state ( $g_1$  or  $g_2$ ) but also by the momentum along the  $z$ -axis:

$$|\psi_D\rangle = c_1 |g_1, -\hbar k_1\rangle + c_2 |g_2, +\hbar k_2\rangle \quad (3)$$

This is due to the fact that  $g_1$  and  $g_2$  must be associated with different

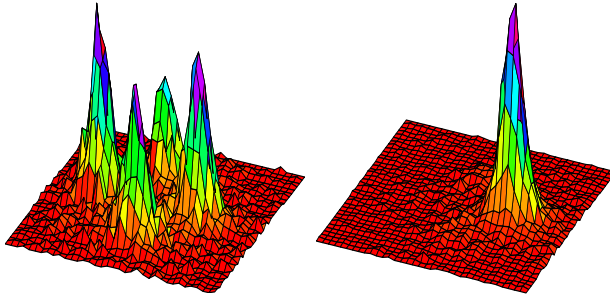


Figure 7: Velocity selective coherent population trapping (VSCPT) in two dimensions with metastable helium atoms (from [44]). The velocity distribution on the left has been obtained using four laser beams in a horizontal plane, giving rise to four peaks located at  $(v_x = \pm v_R, v_y = 0)$  and  $(v_x = 0, v_y = \pm v_R)$ . When three of the four VSCPT beams are adiabatically switched off (right figure), the whole atomic population is transferred into a single wave packet. For a better visibility the vertical scale of the left figure has been expanded by a factor 4 with respect to the right one.

momenta,  $-\hbar k_1$  and  $+\hbar k_2$ , in order to be coupled to the same excited state  $|e_0, p = 0\rangle$  by absorption of photons with different momenta  $+\hbar k_1$  and  $-\hbar k_2$ . Furthermore, when  $\Delta = 0$ , the state (5) is a stationary state of the total atom + laser photons system. As a result of the cooling by VSCPT, the atomic momentum distribution thus exhibits two sharp peaks, centered at  $-\hbar k_1$  and  $+\hbar k_2$ , with a width  $\delta p$  which tends to zero when the interaction time  $\theta$  tends to infinity. Experimentally, temperatures as low as  $T_R/800$  have been observed [40].

VSCPT has been extended to two [41] and three [42] dimensions. For a  $J_g = 1 \leftrightarrow J_e = 1$  transition, it has been shown [43] that there is a dark state which is described by the same vector field as the laser field. More precisely, if the laser field is formed by a linear superposition of  $N$  plane waves with wave vectors  $\mathbf{k}_i$  ( $i = 1, 2, \dots, N$ ) having the same modulus  $k$ , one finds that atoms are cooled in a coherent superposition of  $N$  wave packets with mean momenta  $\hbar \mathbf{k}_i$  and with a momentum spread  $\delta p$  which becomes smaller and smaller as the interaction time  $\theta$  increases. Furthermore, because of the isomorphism between the de Broglie dark state and the laser field, one can adiabatically change the laser configuration and transfer the whole atomic population into a single wave packet chosen at will (Fig. 7).

### 5.3 Subrecoil laser cooling and Lévy statistics

Quantum Monte Carlo simulations using the delay function [45, 46] have provided new physical insight into subrecoil laser cooling [47]. They show

that the random walk of the atom in velocity space is anomalous and dominated by a few rare events whose duration is a significant fraction of the total interaction time. More precisely one can prove that the distribution  $P(\tau)$  of the trapping times  $\tau$  in a small trapping zone near  $v = 0$  is a broad distribution which falls as a power-law in the wings. These wings decrease so slowly that the average value  $\langle \tau \rangle$  of  $\tau$  (or the variance) can diverge. In such cases, the central limit theorem (CLT) can obviously no longer be used for studying the distribution of the total trapping time after  $N$  entries in the trapping zone separated by  $N$  exits.

It is possible to extend the CLT to broad distributions with power-law wings [48]. We have applied the corresponding statistics, called *Lévy statistics*, to subrecoil cooling and shown that one can obtain in this way a better understanding of the physical processes as well as quantitative analytical predictions for the asymptotic properties of the cooled atoms in the limit when the interaction time  $\theta$  tends to infinity [47]. For example, one predicts in this way that the temperature decreases as  $1/\theta$  when  $\theta \rightarrow \infty$ , and that the wings of the momentum distribution decrease as  $1/p^2$ , which shows that the shape of the momentum distribution is closer to a Lorentzian than a Gaussian. This is in agreement with experimental observations [40].

One important feature revealed by this theoretical analysis is the non ergodicity of the cooling process. Regardless of the interaction time  $\theta$ , there are always atomic evolution times (trapping times in the small zone of Fig. 5 around  $v = 0$ ) which can be longer than  $\theta$ . Experimental evidence for non ergodic effects has recently been obtained [49]. Another advantage of such a new approach is that it allows the parameters of the cooling lasers to be optimized for given experimental conditions. For example, by using different shapes for the laser pulses used in one-dimensional subrecoil Raman cooling, it has been possible to reach for Cesium atoms temperatures as low as 3 nK [50].

## 6 Evaporative Cooling and Bose–Einstein Condensation

A spectacular use of cold atom technology has been the demonstration in 1995 of Bose–Einstein condensation (BEC) in a dilute atomic gas. The first gaseous Bose–Einstein condensate has been obtained with rubidium atoms ( $^{87}\text{Rb}$ ) [51]; subsequently BEC has also been demonstrated with sodium [52], lithium [53] and hydrogen [54]. A detailed discussion of this very lively field of research is outside the scope of the present paper, and we refer the interested reader to the reference [55]. In the following we simply outline the basic features of BEC for atomic gases.

BEC has been initially predicted by Einstein in 1925, who was considering an ideal gas of indistinguishable material particles. If the density  $n$  of the

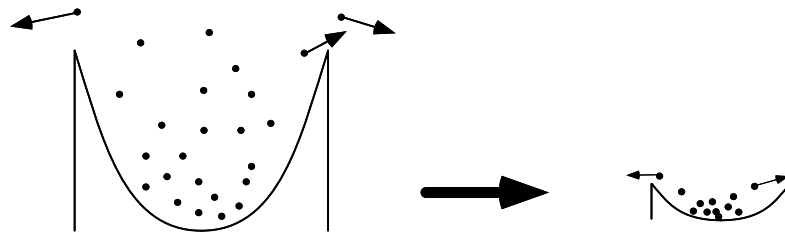


Figure 8: Principle of forced evaporative cooling. Atoms are confined in a truncated potential well (in practice a magnetic trap), whose depth is a few times larger than the thermal energy  $k_B T$ . The fastest atoms are ejected, while the remaining atoms thermalize to a lower temperature. The truncation value is decreased accordingly, to maintain a constant evaporation rate.

gas is larger than the critical value

$$n_c \simeq \frac{0,166}{\hbar^3} (mk_B T)^{3/2} \quad (4)$$

one expects that a macroscopic fraction of atoms condense in the quantum ground state of the box confining the gas. For a long period, the only experimental example of a Bose-Einstein condensate has been liquid helium, below the superfluid transition temperature. However this dense system is far from Einstein's ideal gas model. For instance due to the interactions within the liquid, the condensed fraction never exceeds 10% of the atoms, while it should reach 100% at zero temperature for an ideal gas. Therefore numerous efforts have been made to achieve BEC with dilute systems, closer to the initial model.

Laser cooled and trapped atoms were *a priori* good candidates for observing the condensation phenomenon. Unfortunately, it has not been possible to increase the atomic density in these samples to the value given in Eq. (4). Up to now, light-assisted inelastic collisions between laser cooled atoms have limited the density to a small fraction only of  $n_c$ . As a consequence the realization of BEC with Li, Na and Rb uses laser cooling and trapping only as first step. The atoms are then transferred into a magnetic trap, formed around a magnetic field minimum, which confines the atoms whose magnetic moment is anti-parallel with the local magnetic field. To increase further the density and decrease the temperature, one then proceeds with forced evaporative cooling.

Evaporative cooling consists in using a truncated confining magnetic potential, so that the fastest atoms are ejected from the trap (see fig. 8). Due to elastic collisions, the remaining atoms reach a lower temperature. In practice the truncation of the potential is chosen 5 to 6 times larger than

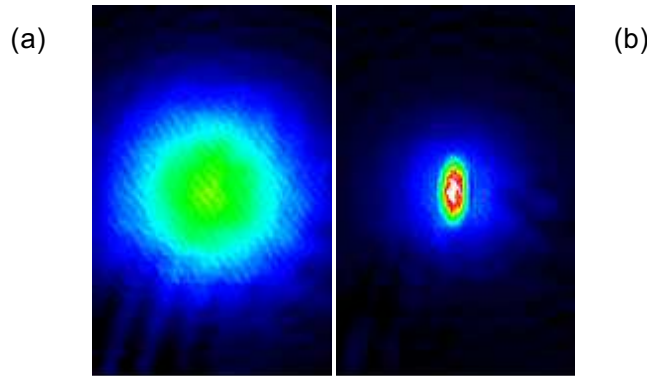


Figure 9: Velocity distributions of a  $^{87}\text{Rb}$  gas. Both pictures represent the absorption of a probe laser beam by the cloud after a 31 ms free fall. (a) Temperature above condensation: isotropic velocity distribution. (b) Temperature below condensation: the anisotropic central feature corresponds to a macroscopically occupied ground state (figure obtained at ENS by P. Desbiolles, D. Guéry-Odelin and J. Söding).

the instantaneous thermal energy  $k_{\text{B}}T$ , and one lowers this truncation continuously as the remaining atoms get colder. Typically a reduction of the temperature by a factor 1000, and an increase of the density by a factor 30 is obtained through the evaporation of 99.9% of the atoms. One starts with  $\sim 10^9$  atoms at a temperature of  $\sim 1$  mK, and ends up at the condensation point with  $10^6$  atoms at  $1 \mu\text{K}$  (see Fig. 9).

Since the first realization of an atomic BEC, there has been numerous experimental and theoretical studies of these systems: phase coherence properties, superfluidity, excitation spectra, non linear atom optics (see [55] for a review). In direct relation with the topic of this book, pulsed diffraction limited and coherent atomic beams have been generated, using these condensates as a source [56]. These beams are often referred to as “atom lasers”, to emphasize the analogy between them and the coherent light beams issued from a laser device. There is no doubt that these coherent atomic sources will play a crucial role in future precision experiments dealing with atom optics and interferometry, metrology, or nanolithography.

## 7 Cold atom clocks

Cesium atoms cooled by Sisyphus cooling have an effective temperature on the order of  $1 \mu\text{K}$ , corresponding to a r.m.s. velocity of  $1 \text{ cm s}^{-1}$ . This allows them to spend a longer time  $T$  in an observation zone where a microwave

field induces resonant transitions between the two hyperfine levels  $g_1$  and  $g_2$  of the ground state. Increasing  $T$  decreases the width  $\Delta\nu \sim 1/T$  of the microwave resonance line whose frequency is used to define the unit of time. The stability of atomic clocks can thus be considerably improved by using ultracold atoms [57, 58].

In usual atomic clocks, atoms from a thermal cesium beam cross two microwave cavities fed by the same oscillator. The average velocity of the atoms is several hundred  $\text{m s}^{-1}$ , the distance between the two cavities is on the order of 1 m. The microwave resonance between  $g_1$  and  $g_2$  is monitored and is used to lock the frequency of the oscillator to the center of the atomic line. The narrower the resonance line, the more stable the atomic clock. In fact, the microwave resonance line exhibits Ramsey interference fringes whose width  $\Delta\nu$  is determined by the time of flight  $T$  of the atoms from one cavity to another. For the longest devices,  $T$ , which can be considered as the observation time, can reach 10 ms, leading to values of  $\Delta\nu \sim 1/T$  on the order of 100 Hz.

Much narrower Ramsey fringes, with sub-Hertz linewidths can be obtained in the so-called *Zacharias atomic fountain* [59]. Atoms are captured in a magneto-optical trap and laser cooled before being launched upwards by a laser pulse through a microwave cavity. Because of gravity they are decelerated, they return and fall back, passing a second time through the cavity. Atoms therefore experience two coherent microwave pulses, when they pass through the cavity, the first time on their way up, the second time on their way down. The time interval between the two pulses can now be on the order of 1 sec, *i.e.* about two order of magnitudes longer than with usual clocks. Atomic fountains have been realized for sodium [60] and cesium [61]. A short-term relative frequency stability of  $4 \times 10^{-14} \tau^{-1/2}$ , where  $\tau$  is the integration time, has been recently measured for a one meter high Cesium fountain [62]. This stability reaches now the fundamental quantum noise induced by the measurement process: it varies as  $N^{-1/2}$ , where  $N$  is the number of detected atoms. The long term stability of  $6 \times 10^{-16}$  is most likely limited by the Hydrogen maser which is used as a reference source. The real fountain stability, which will be more precisely determined by beating the signals of two fountain clocks, is expected to reach  $\Delta\nu/\nu \sim 10^{-16}$  for a one day integration time. In addition to the stability, another very important property of a frequency standard is its accuracy. Because of the very low velocities in a fountain device, many systematic shifts are strongly reduced and can be evaluated with great precision. With an accuracy of  $2 \times 10^{-15}$ , the BNM-LPTF fountain is presently the most accurate primary standard [63]. A factor 10 improvement in this accuracy is expected in the near future. In addition cold atom clocks designed for a reduced gravity environment are currently being built and tested, in order to increase the observation time beyond one second [64]. These clocks should operate in space in relatively near future.

## References

- [1] A more detailed presentation can be found with the text of the three Nobel lectures of 1997: S. Chu, Rev. Mod. Phys. **70**, 685 (1998), C. Cohen-Tannoudji, Rev. Mod. Phys. **70**, 707 (1998), and W.D. Phillips, Rev. Mod. Phys. **70**, 721 (1998).
- [2] A. Kastler, J. Phys. Rad. **11**, 255 (1950).
- [3] For a historical survey of this research field, we refer the reader to the following review papers: A. Ashkin, Science, **210**, 1081 (1980); V.S. Letokhov and V.G. Minogin, Phys.Reports, **73**, 1 (1981); S. Stenholm, Rev.Mod.Phys. **58**, 699 (1986); C.S. Adams and E. Riis, Prog. Quant. Electr. **21**, 1 (1997).
- [4] C. Cohen-Tannoudji and W. Phillips, Physics Today **43**, No 10, 35 (1990).
- [5] C. Cohen-Tannoudji, J. Dupont-Roc and G. Grynberg, *Atom-photon interactions – Basic processes and applications*, (Wiley, New York, 1992).
- [6] J.V. Prodan, W.D. Phillips and H. Metcalf, Phys. Rev. Lett. **49**, 1149 (1982).
- [7] W. Ertmer, R. Blatt, J.L. Hall and M. Zhu, Phys. Rev. Lett. **54**, 996 (1985).
- [8] C. Cohen-Tannoudji, *Atomic motion in laser light*, in *Fundamental systems in quantum optics*, J. Dalibard, J.-M. Raimond, and J. Zinn-Justin eds, Les Houches session LIII (1990), (North-Holland, Amsterdam 1992) p.1.
- [9] J. Dalibard and C. Cohen-Tannoudji, J.Opt.Soc.Am. **B2**, 1707 (1985).
- [10] T.W. Hänsch and A.L. Schawlow, Opt. Commun. **13**, 68 (1975).
- [11] D. Wineland and H. Dehmelt, Bull. Am. Phys. Soc. **20**, 637 (1975).
- [12] S. Chu, L. Hollberg, J.E. Bjorkholm, A. Cable and A. Ashkin, Phys. Rev. Lett. **55**, 48 (1985).
- [13] J.P. Gordon and A. Ashkin, Phys. Rev. **A21**, 1606 (1980).
- [14] V.S. Letokhov, V.G. Minogin and B.D. Pavlik, Zh. Eksp. Teor. Fiz. **72**, 1328 (1977) [Sov.Phys.JETP, **45**, 698 (1977)].
- [15] D.J. Wineland and W. Itano, Phys.Rev. **A20**, 1521 (1979).

- [16] P.D. Lett, R.N. Watts, C.I. Westbrook, W. Phillips, P.L. Gould and H.J. Metcalf, *Phys. Rev. Lett.* **61**, 169 (1988).
- [17] E.L. Raab, M. Prentiss, A. Cable, S. Chu and D.E. Pritchard, *Phys.Rev.Lett.* **59**, 2631 (1987).
- [18] C. Monroe, W. Swann, H. Robinson and C.E. Wieman, *Phys.Rev.Lett.* **65**, 1571 (1990).
- [19] V.S. Letokhov, *Pis'ma. Eksp. Teor. Fiz.* **7**, 348 (1968) [*JETP Lett.*, **7**, 272 (1968)].
- [20] S. Chu, J.E. Bjorkholm, A. Ashkin and A. Cable, *Phys.Rev.Lett.* **57**, 314 (1986).
- [21] C.S. Adams, H.J. Lee, N. Davidson, M. Kasevich and S. Chu, *Phys. Rev. Lett.* **74**, 3577 (1995).
- [22] A. Kuhn, H. Perrin, W. Hänsel and C. Salomon, *OSA TOPS on Ultra-cold Atoms and BEC*, 1996, Vol. 7, p.58, Keith Burnett (ed.), (Optical Society of America, 1997).
- [23] R.J. Cook and R.K. Hill, *Opt. Commun.* **43**, 258 (1982).
- [24] V.I. Balykin, V.S. Letokhov, Yu. B. Ovchinnikov and A.I. Sidorov, *Phys. Rev. Lett.* **60**, 2137 (1988).
- [25] M.A. Kasevich, D.S. Weiss and S. Chu, *Opt. Lett.* **15**, 607 (1990).
- [26] C.G. Aminoff, A.M. Steane, P. Bouyer, P. Desbiolles, J. Dalibard and C. Cohen-Tannoudji, *Phys. Rev. Lett.* **71**, 3083 (1993).
- [27] J. Dalibard and C. Cohen-Tannoudji, *J. Opt. Soc. Am.* **B6**, 2023 (1989).
- [28] P.J. Ungar, D.S. Weiss, E. Riis and S. Chu, *JOSA* **B6**, 2058 (1989).
- [29] C. Salomon, J. Dalibard, W. Phillips, A. Clairon and S. Guellati, *Europhys. Lett.* **12**, 683 (1990).
- [30] Y. Castin and K. Mølmer, *Phys. Rev. Lett.* **74**, 3772 (1995).
- [31] Y. Castin and J. Dalibard, *Europhys.Lett.* **14**, 761 (1991).
- [32] P. Verkerk, B. Lounis, C. Salomon, C. Cohen-Tannoudji, J.-Y. Courtois and G. Grynberg, *Phys. Rev. Lett.* **68**, 3861 (1992).
- [33] P.S. Jessen, C. Gerz, P.D. Lett, W.D. Phillips, S.L. Rolston, R.J.C. Spreeuw and C.I. Westbrook, *Phys. Rev. Lett.* **69**, 49 (1992).

- [34] G. Grynberg and C. Triché, in *Proceedings of the International School of Physics Enrico Fermi*, Course CXXXI, A. Aspect, W. Barletta and R. Bonifacio (Eds), p.243, IOS Press, Amsterdam (1996); A. Hemmerich, M. Weidemüller and T.W. Hänsch, same Proceedings, p.503.
- [35] P.S. Jessen and I.H. Deutsch, in *Advances in Atomic, Molecular and Optical Physics*, **37**, 95 (1996), ed. by B. Bederson and H. Walther.
- [36] A. Aspect, E. Arimondo, R. Kaiser, N. Vansteenkiste, and C. Cohen-Tannoudji, *Phys. Rev. Lett.* **61**, 826 (1988).
- [37] M. Kasevich and S. Chu, *Phys. Rev. Lett.* **69**, 1741 (1992).
- [38] G. Alzetta, A. Gozzini, L. Moi, G. Orriols, *Il Nuovo Cimento* **36B**, 5 (1976); Arimondo E., Orriols G., *Lett. Nuovo Cimento* **17**, 333 (1976).
- [39] A. Aspect, E. Arimondo, R. Kaiser, N. Vansteenkiste, and C. Cohen-Tannoudji, *J. Opt. Soc. Am.* **B6**, 2112 (1989).
- [40] B. Saubamea, T.W. Hijmans, S. Kulin, E. Rasel, E. Peik, M. Leduc and C. Cohen-Tannoudji, *Phys. Rev. Lett.* **79**, 3146 (1997).
- [41] J. Lawall, F. Bardou, B. Saubamea, K. Shimizu, M. Leduc, A. Aspect and C. Cohen-Tannoudji, *Phys. Rev. Lett.* **73**, 1915 (1994).
- [42] J. Lawall, S. Kulin, B. Saubamea, N. Bigelow, M. Leduc and C. Cohen-Tannoudji, *Phys. Rev. Lett.* **75**, 4194 (1995).
- [43] M.A. Ol'shania and V.G. Minogin, *Opt.Comm.* **89**, 393 (1992).
- [44] S. Kulin, B. Saubamea, E. Peik, J. Lawall, T.W. Hijmans, M. Leduc and C. Cohen-Tannoudji, *Phys. Rev. Lett.* **78**, 4185 (1997).
- [45] C. Cohen-Tannoudji and J. Dalibard, *Europhys. Lett.* **1**, 441 (1986).
- [46] P. Zoller, M. Marte and D.F. Walls, *Phys. Rev.* **A35** 198 (1987).
- [47] F. Bardou, J.-P. Bouchaud, O. Emile, A. Aspect and C. Cohen-Tannoudji, *Phys. Rev. Lett.* **72** 203 (1994).
- [48] J.P. Bouchaud and A. Georges, *Phys. Rep.* **195**, 127 (1990).
- [49] B. Saubamea, M. Leduc, and C. Cohen-Tannoudji, *Phys. Rev. Lett.* **83**, 3796 (1999).
- [50] J. Reichel, F. Bardou, M. Ben Dahan, E. Peik, S. Rand, C. Salomon and C. Cohen-Tannoudji, *Phys. Rev. Lett.* **75**, 4575 (1995).
- [51] M. H. Anderson, J. Ensher, M. Matthews, C. Wieman, and E. Cornell, *Science* **269**, 198 (1995).

- [52] K. B. Davis, M.O. Mewes, N. Van Druten, D. Durfee, D. Kurn, and W. Ketterle, *Phys. Rev. Lett.* **75**, 3969 (1995).
- [53] C. C. Bradley, C. A. Sackett, and R. G. Hulet, *Phys. Rev. Lett.* **78**, 985 (1997); see also C. C. Bradley, C. A. Sackett, J. J. Tollett, and R. G. Hulet, *Phys. Rev. Lett.* **75**, 1687 (1995).
- [54] D. Fried, T. Killian, L. Willmann, D. Landhuis, S. Moss, D. Kleppner, and T. Greytak, *Phys. Rev. Lett.* **81**, 3811 (1998).
- [55] M. Inguscio, S. Stringari, and C.E. Wieman, *Proceedings of the International School of Physics Enrico Fermi, Course CXL, Bose-Einstein Condensation in Atomic Gases* (IOS Press, Amsterdam, 1999).
- [56] K. Helmerson, D. Hutchinson, K. Burnett and W. D. Phillips, *Atom lasers*, *Physics World*, August 1999, p. 31; Y. Castin, R. Dum and A. Sinatra, *Bose condensates make quantum leaps and bounds*, *Physics World*, August 1999, p. 37.
- [57] K. Gibble and S. Chu, *Metrologia*, **29**, 201 (1992).
- [58] S.N. Lea, A. Clairon, C. Salomon, P. Laurent, B. Lounis, J. Reichel, A. Nadir, and G. Santarelli, *Physica Scripta* **T51**, 78 (1994).
- [59] J. Zacharias, *Phys. Rev.* **94**, 751 (1954). See also : N. Ramsey, *Molecular Beams*, Oxford University Press, Oxford, 1956.
- [60] M. Kasevich, E. Riis, S. Chu and R. de Voe, *Phys. Rev. Lett.* **63**, 612 (1989).
- [61] A. Clairon, C. Salomon, S. Guellati and W.D. Phillips, *Europhys. Lett.* **16**, 165 (1991).
- [62] G. Santarelli, Ph. Laurent, P. Lemonde, A. Clairon, A. G. Mann, S. Chang, A. N. Luiten, and C. Salomon, *Phys. Rev. Lett.* **82**, 4619 (1999).
- [63] E. Simon, P. Laurent, C. Mandache and A. Clairon, *Proceedings of EFTF 1997*, Neuchatel, Switzerland.
- [64] Ph. Laurent, P. Lemonde, E. Simon, G. Santarelli, A. Clairon, N. Dimarcq, P. Petit, C. Audoin, and C. Salomon, *Eur. Phys. J. D* **3**, 201 (1998).